

Article

# Tuning the Resonant Frequency of a Surface Plasmon by Double-Metallic Ag/Au Nanoparticles for High-Efficiency Green Light-Emitting Diodes

Ryoya Mano <sup>1</sup>, Dong-Pyo Han <sup>1,\*</sup>, Kengo Yamamoto <sup>1</sup>, Seiji Ishimoto <sup>1</sup>, Satoshi Kamiyama <sup>1</sup>, Tetsuya Takeuchi <sup>1</sup>, Motoaki Iwaya <sup>1</sup> and Isamu Akasaki <sup>1,2</sup>

<sup>1</sup> Faculty of Science and Technology, Meijo University, Nagoya 468-8502, Japan; 150443054@ccalumni.meijo-u.ac.jp (R.M.); 130443086@ccalumni.meijo-u.ac.jp (K.Y.); 140443005@ccalumni.meijo-u.ac.jp (S.I.); skami@meijo-u.ac.jp (S.K.); take@meijo-u.ac.jp (T.T.); iwaya@meijo-u.ac.jp (M.I.); akasaki@meijo-u.ac.jp (I.A.)

<sup>2</sup> Akasaki Research Center, Nagoya University, Nagoya 464-8603, Japan

\* Correspondence: han@meijo-u.ac.jp; Tel.: +81-52-838-1151

Received: 26 December 2018; Accepted: 11 January 2019; Published: 16 January 2019



**Abstract:** Currently, the internal quantum efficiency (IQE) of GaInN-based green light-emitting diodes (LEDs) is still low. To overcome this problem, surface plasmon (SP)-enhanced LEDs have been intensively studied for the last 15 years. For an SP effect in green LEDs, Au and Ag are typically employed as the plasmonic materials. However, the resonance wavelength is determined by their material constants, which are theoretically fixed at ~537 nm for Au and ~437 nm for Ag. In this study, we aimed to tune the SP resonant wavelength using double-metallic nanoparticles (NPs) composed of Au and Ag to match the SP resonance wavelength to the LED emission wavelength to consequently improve the IQE of green LEDs. To form double-metallic NPs, Au/Ag multilayers were deposited on a GaN layer and then thermally annealed. We changed the thicknesses of the multilayers to control the Ag/Au ratio in the NPs. We show that the SP resonant wavelength could be tuned using our approach. We also demonstrate that the enhancement of the IQE in SP-enhanced LEDs was strongly dependent on the SP resonant wavelength. Finally, the highest IQE was achieved by matching the SP resonant wavelength to the LED emission wavelength.

**Keywords:** light-emitting diode; surface plasmon; resonant frequency; internal quantum efficiency; nanoparticle

## 1. Introduction

During the last few decades, tremendous developments in GaInN-based light-emitting diodes (LEDs) have been achieved, e.g., epitaxial growth, fabrication, packaging, and physics in optoelectronic devices [1,2]. Hence, they are currently utilized in various places, including full-color displays, traffic signals, and mobile phones, with the advantages of a long lifetime, small size, high brightness, environmental friendliness, and low power consumption [3,4]. They are even considered to be candidates for a next-generation general white light source. Currently, the external quantum efficiency (EQE) of this material system at blue emission wavelengths is above 80%. However, when moving toward long wavelengths by increasing the indium (In) composition in the multiple quantum wells (MQWs) active region, the EQE drastically decreases, i.e., ~50% for green emission wavelengths and ~20% for yellow emission wavelengths [5,6]. This is the so-called “green-gap” problem described by researchers. This is fundamentally due to problems such as the low crystal quality of GaInN layers with a high In composition [7], strong polarization-induced electric fields in highly strained GaInN-based MQWs [8], and alloy fluctuation-induced carrier localization [9]. With these problems, the nonradiative

recombination rate increases, and the radiative recombination rate decreases as the In content in MQWs increases. Consequently, the internal quantum efficiency (IQE) decreases. Accordingly, there are two possible approaches to increasing the IQEs of green LEDs, i.e., decreasing the nonradiative recombination rate and/or increasing the radiative recombination rate. For instance, improving crystal quality via the reduction of the threading dislocation density is one method of increasing the IQE by decreasing the nonradiative recombination rate [10], and controlling the quantum confined stark effect in MQWs via strain relaxation is another possible method of increasing the IQE by increasing the radiative recombination rate [11].

Among the several methods of increasing the IQE of GaInN-based LEDs, surface plasmon (SP) coupling with excitons in MQWs has been intensively studied over the last 15 years as a way to increase the radiative recombination rate [12–19]. SPs are the collective oscillations of free electrons in metals at the interfaces between metals and dielectrics. SPs excited by the interaction between light and metal surfaces can enhance the recombination rate and increase Raman scattering intensities. When the resonance frequency of the surface plasmon polaritons (SPPs) overlaps with the emission frequency of the MQWs at the metal and semiconductor interface, the MQW energy can transfer to the SPs. Consequently, this new path of recombination increases the spontaneous radiative recombination rate, and the IQE thus increases. Thus, this is an approach to improve IQEs by increasing the radiative recombination rate rather than by decreasing the nonradiative recombination rate. From this point of view, the IQEs of conventional LEDs (Equation (1)) and of SP-enhanced LEDs (Equation (2)) are given by [20,21]

$$\eta_{IQE} = \frac{R_R}{R_R + R_{NR}}, \quad (1)$$

$$\eta_{IQE\_SP} = \frac{R_R + R_{SPC} \cdot C_{ext}}{R_R + R_{NR} + R_{SPC}}, \quad (2)$$

where  $R_R$ ,  $R_{NR}$ ,  $R_{SPC}$ , and  $C_{ext}$  are the radiative recombination rate, the nonradiative recombination rate, the SP coupling rate, and the probability of photon extraction from the SP energy, respectively. From these definitions in Equations (1) and (2), we can observe that when the  $R_{SPC}$  is much greater than  $R_R$  and  $R_{NR}$ , the IQE of an SP-enhanced LED drastically increases. To obtain a higher  $R_{SPC}$  for SP-enhanced LEDs, it is of prime importance to match the resonance frequency of the SPPs to the emission frequency of the MQWs.

In GaInN-based SP-enhanced LEDs, Al, Ag, and Au thin films are typically used as plasmonic materials. The resonance frequencies of the SPPs for Al, Ag, and Au thin films on the GaN layer, i.e., Al/GaN, Ag/GaN, and Au/GaN, correspond to ~5.1 eV (~243 nm), ~2.8 eV (~442 nm), and ~2.3 eV (~539 nm), respectively [21]. Since the resonance frequency of the SPPs is determined by the material constant, matching the resonance frequency of the SPPs to the emission frequency of the MQWs is fundamentally impossible with a single plasmonic material. To overcome this problem, there have been efforts to tune the resonance frequency of SPPs via double-metallic Au/Ag multiple layers [22], Ag/Si<sub>3</sub>N<sub>4</sub>/Au multiple layers [23], Ag/ZnO/Au multiple layers [24], and Ag/TiO<sub>2</sub>/Au multiple layers [25]. Furthermore, double-metallic NPs are frequently employed in such devices as sensors [26], solar cells [27], and lasers [28] to improve their performance.

In practice, it is difficult to realize SP-enhanced LEDs covered with a thin metal film deposited on the device surface because photons typically are emitted into the free space via the device surface. For this reason, SP-enhanced LEDs covered with self-assembled nanoparticles (NPs) on top of a p-GaN layer are often studied [29–33]. In this case, the collective oscillations of electrons in randomly distributed metal NPs coupled with excitons in MQWs occur via localized surface plasmon (LSP) modes. In particular, the resonant frequency is dependent on the shape and size of NPs in LSP modes. However, the control of their shape and size to tune the resonant frequency is very difficult now.

In this paper, to obtain a high value of  $R_{SPC}$  and to improve IQEs in SP-enhanced LEDs, we attempted to match the resonance frequency of LSPs to the emission frequency of MQWs by tuning the resonance frequency of LSPs. To tune the resonance frequency of LSPs, we used double-metallic

Ag/Au NPs prepared via thermal annealing of double-metallic Ag/Au multilayers. To control the Ag/Au ratio in the NPs, we carefully changed the thickness of the double-metallic Ag/Au multilayers. Then, we measured the absorption spectrum to investigate the LSP resonance energy. The enhancement factors (EFs) (i.e., the enhancement ratio of the luminescence efficiency in an SP-enhanced LED to that of a conventional LED) of the photoluminescence (PL) efficiency of green LEDs were measured to confirm IQE improvement using this approach.

## 2. Experiments

We prepared two groups of samples. Group 1 was for measuring the resonant frequency of the LSPs, i.e., a 4- $\mu\text{m}$ -thick undoped GaN (u-GaN) layer sample grown by metal–organic chemical vapor deposition (MOCVD) on a *c*-sapphire substrate. Group 2 was for measuring the EFs in the SP-LEDs, i.e., green InGaN/GaN LEDs grown via MOCVD in which the epi-structure of the sample consisted of a 30-nm-thick low temperature GaN buffer layer, a 4- $\mu\text{m}$ -thick u-GaN template layer, a Si-doped n- $\text{Al}_{0.025}\text{Ga}_{0.975}\text{N}$  layer, 10 pairs of GaN/ $\text{In}_{0.05}\text{Ga}_{0.95}\text{N}$  superlattices (SLs), and 5 pairs of MQWs composed of a 3-nm-thick QW sandwiched between 15-nm-thick GaN barriers. On top of the MQWs, a 100-nm-thick Mg-doped p-GaN layer was grown. Then, the Ag thin film and Au thin film multilayers were sequentially deposited on top of the u-GaN layer for Group 1 and on p-GaN for Group 2 via electron beam evaporation in an identical manner. To form the self-assembled double-metallic NPs, all the samples were thermally annealed using a rapid thermal annealing system in  $\text{N}_2$  atmosphere for 10 min at 250 °C. Figure 1a,b shows a schematic illustration of the process of sample preparation. Here, we changed the thickness of the Ag and Au thin film layers to control the ratio of Ag to Au in the NPs. We fixed the total thickness of the Ag/Au multilayer to 4 nm to maintain similarly sized double-metallic NPs for each sample. Table 1 summarizes detailed information of the deposited Ag and Au layer thicknesses required to form the self-assembled double-metallic NPs.

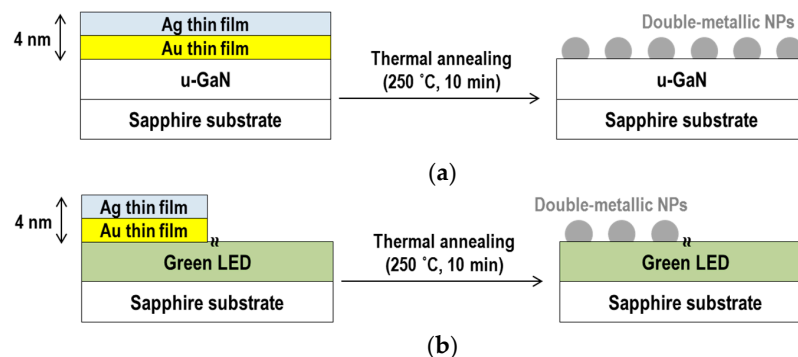


**Figure 1.** Schematic illustrations of the sample preparation process. (a) Double-metallic nanoparticles (NPs) on an undoped GaN (u-GaN) layer for measuring the resonant frequency of localized surface plasmon (LSP) modes. (b) Double-metallic NPs on a green light-emitting diode (LED) for measuring the enhancement factor (EF) of the photoluminescence (PL) intensity.

**Table 1.** Thicknesses of Au/Ag multilayers to form the double-metallic NPs.

Sample	Ag Thickness	Au Thickness
NPs 1	4 nm	-
NPs 2	3 nm	1 nm
NPs 3	2 nm	2 nm
NPs 4	1 nm	3 nm
NPs 5	-	4 nm

## 3. Results and Discussions

Figure 2a–e shows top view scanning electron microscope (SEM) images of the self-assembled double-metallic NPs (NPs 1, NPs 2, NPs 3, NPs 4, and NPs 5) on the u-GaN layer, respectively. The NP

sizes were all similar for all samples except for NPs 1. More specifically, the average diameter of the NPs was estimated to be  $\sim 33$  nm for NPs 1, but  $\sim 40$  nm for the others. From the analysis given in References [34,35], the resonant frequency of the LSPs is strongly dependent on the size and density of the NPs. Thus, in this study, we took into account only the Ag/Au ratio of the NPs, regardless of the size or density effects of the NPs.

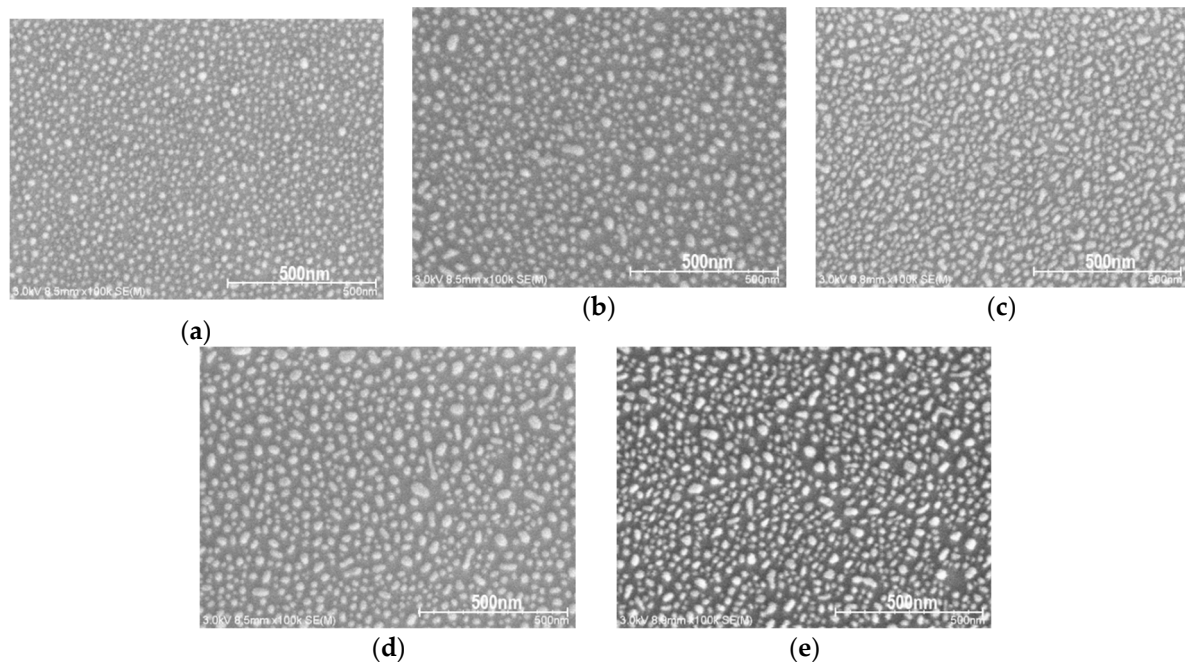


**Figure 2.** Top view SEM images of (a) NPs 1 on the u-GaN layer, (b) NPs 2 on the u-GaN layer, (c) NPs 3 on the u-GaN layer, (d) NPs 4 on the u-GaN layer, and (e) NPs 5 on the u-GaN layer.

Figure 3a shows the absorption spectra for NPs 1, NPs 2, NPs 3, NPs 4, and NPs 5 on the u-GaN layer, as shown in Figure 1a. The absorption spectra are strongly dependent on the Ag/Au ratio in double-metallic NPs. Because the resonant wavelength of the LSP mode corresponds to the wavelength at peak absorption, the resonant wavelength of the LSP mode for each NP can be obtained, and are plotted in Figure 3b as a function of the ratio of Ag film thickness to total film thickness, i.e., Ag film thickness/4 nm. The dashed line is the fifth-order polynomial fitting curve. The data fit very well. The inset picture in Figure 3b shows different colored samples due to the different absorption characteristics of each NP. The resonant wavelength of the LSP mode for NPs 1, which was composed of only Ag, corresponded to  $\sim 516$  nm, whereas that of NPs 5, which was composed of only Au, corresponded to  $\sim 630$  nm. These values were similar to those obtained in previous research reports [35,36]. Additionally, the resonant wavelength of the LSP mode can be tuned by adjusting the ratio of Ag to Au in the NPs within the wavelength range of 516 nm to 630 nm. Thus, we could match the resonant wavelength of the LSP to green- and yellow-emitting LEDs by tuning them. In addition, when the Ag NPs and Au NPs were separately formed, dual peaks in the absorption spectrum were observed, i.e., one corresponding to Ag NPs and the other corresponding to Au NPs, as presented in Reference [36]. However, we observed only a single peak in the absorption spectrum, as shown in Figure 3a. This implies that Au and Ag were well mixed and that the formed NPs were double-metallic.

To investigate the effect of LSPs on PL efficiency, we measured the PL spectrum of the LED without NPs (reference), the LED with NPs 1, the LED with NPs 2, the LED with NPs 3, the LED with NPs 4, and the LED with NPs 5. For external optical pumping, a 405-nm laser diode was used, and the peak PL wavelength of the reference was approximately 528 nm. Figure 4a shows the PL spectra for the samples, and Figure 4b shows the EFs, i.e., the integrated PL intensities of the SP-enhanced LEDs over the integrated PL intensities of the conventional LED for the samples. Note that the PL intensities in

Figure 4a depended on the measurement location, and the difference was about 5% to 7%. As Figure 4b shows, the highest EF was observed in the LED with NPs 2. We believe that this was because the peak PL wavelength was closest to the LSP resonant frequency of NPs 2. Namely, the value of  $R_{SPC}$  in Equation (2) increased when the peak PL wavelength was the closest to the LSP resonant frequency, and thus, the IQE increased. In contrast, the value of  $R_{SPC}$  in Equation (2) decreased when the peak PL wavelength was different from the LSP resonant frequency, and thus, the IQE decreased (e.g., from the EF of the LED with NPs 2 to the EF of the LED with NPs 5 in Figure 4b). Therefore, we conclude that LSP resonant frequency can be tuned using our proposed method, and the EF and IQE can be consequently increased by tuning in the green-yellow emission region of a GaInN-based LED.

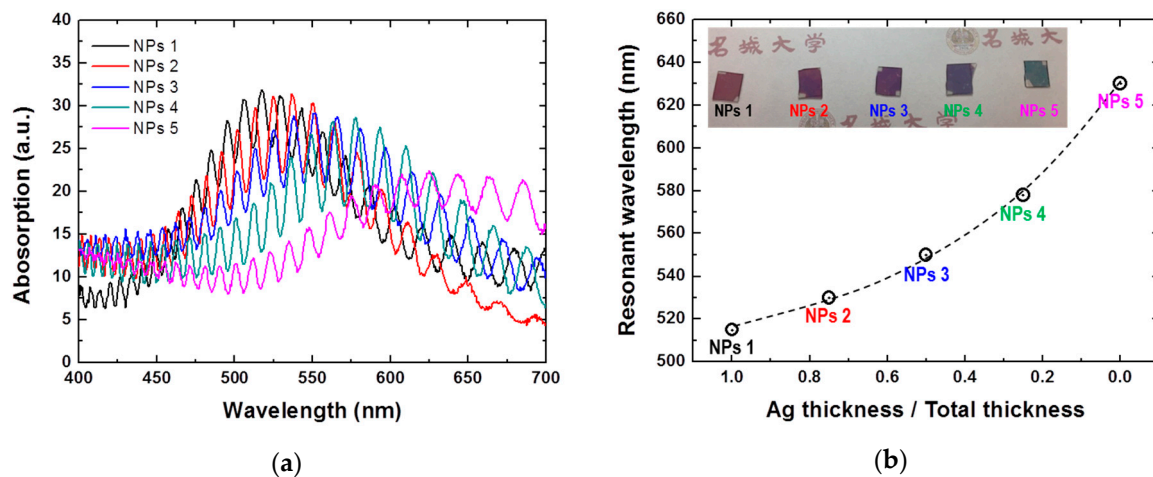


**Figure 3.** (a) Absorption spectra for NPs 1, NPs 2, NPs 3, NPs 4, and NPs 5 on the u-GaN layer and (b) the resonant wavelengths of the LSP modes for NPs 1, NPs 2, NPs 3, NPs 4, and NPs 5 on the u-GaN layer. The inset picture shows different colored samples due to the different absorption characteristics of each NP.

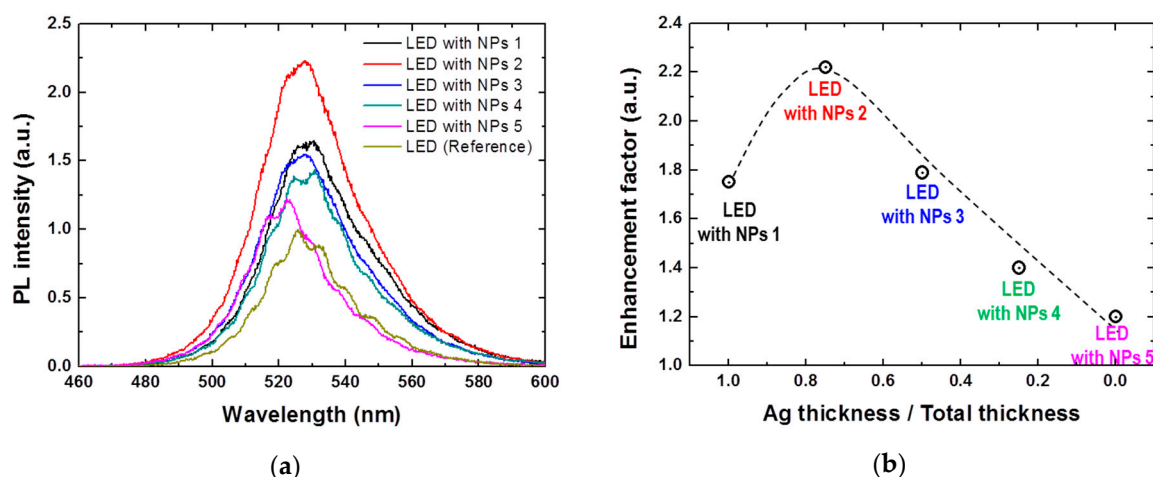


**Figure 4.** (a) PL spectra of the LED without NPs (reference), the LED with NPs 1, the LED with NPs 2, the LED with NPs 3, the LED with NPs 4, and the LED with NPs 5. (b) The enhancement factors of the LED with NPs 1, the LED with NPs 2, the LED with NPs 3, the LED with NPs 4, and the LED with NPs 5.

#### 4. Conclusions

In this study, the use of Au/Ag double-metallic NPs on top of green LEDs was proposed and demonstrated to tune the resonant wavelength of an LSP. To form self-assembled double-metallic NPs,

we deposited a double-metallic multilayer and then thermally annealed it. In particular, by adjusting the thickness of the multilayer, the Au/Ag ratio in the NPs was controlled. Consequently, we showed that the highest EFs and IQE were achieved when the LSP resonant wavelength was identical to the LED emission wavelength. This approach, i.e., LSP resonant wavelength tuning using double-metallic Au/Ag NPs, can be applied to LEDs with wavelengths from ~510 nm to ~640 nm. This approach shows the potential of realizing SP-enhanced LEDs and of overcoming the green gap via an enhanced IQE by matching the LSP resonant wavelength to the emission wavelength of the LED.

**Author Contributions:** R.M., K.Y., S.I., and D.-P.H. conducted the experiments and data analysis under the advising of S.K., T.T., M.I., and I.A., and D.-P.H. and R.M. mainly wrote the manuscript. S.K. read, edited, and commented on the manuscript.

**Funding:** This research was supported by the MEXT Private University Research Branding Project and JSPS KAKENHI for Innovative Areas [No. 16H06416].

**Acknowledgments:** This work was supported by the MEXT Private University Research Branding Project, MEXT Program for research and development of a next-generation semiconductor to realize an energy-saving society, JSPS KAKENHI for Scientific Research A [No. 15H02019], JSPS KAKENHI for Scientific Research A [No. 17H01055], JSPS KAKENHI for Innovative Areas [No. 16H06416], and Japan Science and Technology CREST [No. 16815710].

**Conflicts of Interest:** The authors declare no conflicts of interest.

## References

1. Akasaki, I.; Amano, H. Crystal growth and conductivity control of group III nitride semiconductors and their application to short wavelength light emitters. *Jpn. J. Appl. Phys.* **1997**, *36*, 5393–5408. [[CrossRef](#)]
2. Amano, H. Nobel lecture: Growth of GaN on sapphire via low-temperature deposited buffer layer and realization of *p*-type GaN by Mg doping followed by low-energy electron beam irradiation. *Rev. Mod. Phys.* **2015**, *87*, 1133–1138. [[CrossRef](#)]
3. Akasaki, I. Nobel lecture: Fascinated journeys into blue light. *Rev. Mod. Phys.* **2015**, *87*, 1119–1131. [[CrossRef](#)]
4. Riechert, H. Lighting the 21st century. *Phys. Status Solidi A* **2015**, *212*, 893–896. [[CrossRef](#)]
5. Saito, S.; Hashimoto, R.; Hwang, J.; Nunoue, S. InGaN light-emitting diodes on *c*-face sapphire substrates in green gap spectral range. *Appl. Phys. Express* **2013**, *6*, 111004. [[CrossRef](#)]
6. Crawford, M.H. LEDs for solid-state lighting: Performance challenges and recent advances. *IEEE J. Quantum Electron.* **2009**, *15*, 1028–1040. [[CrossRef](#)]
7. Iida, D.; Kondo, Y.; Sowa, M.; Sugiyama, T.; Iwaya, M.; Takeuchi, T.; Kamiyama, S.; Akasaki, I. Analysis of strain relaxation process in GaInN/GaN heterostructure by in situ X-ray diffraction monitoring during metalorganic vapor-phase epitaxial growth. *Phys. Status Solidi RRL* **2013**, *7*, 211–214. [[CrossRef](#)]
8. Iida, D.; Niwa, K.; Kamiyama, S.; Ohkawa, K. Demonstration of InGaN-based orange LEDs with hybrid multiple-quantum-wells structure. *Appl. Phys. Express* **2016**, *9*, 111003. [[CrossRef](#)]
9. Karpov, S.Y. Effect of carrier localization on recombination processes and efficiency of InGaN-based LEDs operating in the “Green Gap”. *Appl. Sci.* **2018**, *8*, 818. [[CrossRef](#)]
10. Liu, M.; Zhao, J.; Zhou, S.; Gao, Y.; Hu, J.; Liu, X.; Ding, X. An InGaN/GaN superlattice to enhance the performance of green LEDs: Exploring the role of V-pits. *Nanomaterials* **2018**, *8*, 450. [[CrossRef](#)]
11. Doi, T.; Honda, Y.; Yamaguchi, M.; Amano, H. Strain-compensated effect on the growth of InGaN/AlGaIn multi-quantum well by metalorganic vapor phase epitaxy. *Jpn. J. Appl. Phys.* **2013**, *52*, 08JB14. [[CrossRef](#)]
12. Okamoto, K.; Niki, I.; Shvartser, A.; Narukawa, Y.; Mukai, T.; Scherer, A. Surface-plasmon-enhanced light emitters based on InGaN quantum wells. *Nat. Mater.* **2004**, *3*, 601–605. [[CrossRef](#)]
13. Oh, T.S.; Jeong, H.; Lee, Y.S.; Kim, J.D.; Seo, T.H.; Kim, H.; Park, A.H.; Lee, K.J.; Suh, E.-H. Coupling of InGaN/GaN multi-quantum-wells photoluminescence to surface plasmons in platinum nanocluster. *Appl. Phys. Lett.* **2009**, *95*, 111112.
14. Chen, C.-Y.; Yeh, D.-M.; Lu, Y.-C.; Yang, C.C. Dependence of resonant coupling between surface plasmons and an InGaN quantum well on metallic structure. *Appl. Phys. Lett.* **2006**, *89*, 203113. [[CrossRef](#)]
15. Cho, C.-Y.; Kim, K.S.; Lee, S.-J.; Kwon, M.-K.; Ko, H.; Kim, S.-T.; Jung, G.-Y.; Park, S.-J. Surface plasmon-enhanced light-emitting diodes with silver nanoparticles and SiO<sub>2</sub> nano-disks embedded in *p*-GaN. *Appl. Phys. Lett.* **2011**, *99*, 041107. [[CrossRef](#)]

16. Okamoto, K.; Niki, I.; Shvartser, A.; Maltezos, G.; Narukawa, Y.; Mukai, T.; Kawakami, Y.; Scherer, A. Surface plasmon enhanced bright light emission from InGaN/GaN. *Phys. Status Solidi A* **2007**, *204*, 2013–2017. [[CrossRef](#)]
17. Gao, N.; Huang, K.; Li, J.; Li, S.; Yang, X.; Kang, J. Surface-plasmon-enhanced deep-UV light emitting diodes based on AlGaIn multi-quantum wells. *Sci. Rep.* **2012**, *2*, 816. [[CrossRef](#)]
18. Kwon, M.-K.; Kim, J.-Y.; Kim, B.-H.; Park, I.-K.; Cho, C.-Y.; Byeon, C.-C.; Park, S.-J. Surface-plasmon-enhanced light-emitting diodes. *Adv. Mater.* **2008**, *20*, 1253–1257. [[CrossRef](#)]
19. Iida, D.; Fadil, A.; Chen, Y.; Ou, Y.; Kopylov, O.; Iwaya, M.; Takeuchi, T.; Kamiyama, S.; Akasaki, I.; Ou, H. Internal quantum efficiency enhancement of GaInN/GaN quantum-well structures using Ag nanoparticles. *AIP Adv.* **2015**, *5*, 097169. [[CrossRef](#)]
20. Okamoto, K. Surface plasmon enhanced solid-state light-emitting devices. In *Nanoscale Photonics and Optoelectronics*; Wang, Z.M., Neogi, A., Eds.; Springer: New York, NY, USA, 2010; pp. 27–46.
21. Okamoto, K.; Funato, M.; Kawakami, Y.; Tamada, K. High-efficiency light emission by exciton–surface-plasmon coupling. *J. Photochem. Photobiol. C Photochem. Rev.* **2017**, *32*, 58–77. [[CrossRef](#)]
22. Zhao, H.; Zhang, J.; Liu, G.; Tansu, N. Surface plasmon dispersion engineering via double-metallic Au/Ag layers for III-nitride based light-emitting diodes. *Appl. Phys. Lett.* **2011**, *98*, 151115. [[CrossRef](#)]
23. Paiella, R. Tunable surface plasmons in coupled metallo-dielectric multiple layers for light-emission efficiency enhancement. *Appl. Phys. Lett.* **2005**, *87*, 111104. [[CrossRef](#)]
24. Hong, R.; Ji, J.; Tao, C.; Zhang, D. Tunable surface plasmon resonance frequency of Au-Ag bimetallic asymmetric structure thin films in the UV and IR. *Proc. SPIE* **2016**, *10154*, 101548.
25. Henson, J.; Bhattacharyya, A.; Moustakas, T.D.; Paiella, R. Controlling the recombination rate of semiconductor active layers via coupling to dispersion-engineered surface plasmons. *J. Opt. Soc. Am. B* **2008**, *25*, 1328–1335. [[CrossRef](#)]
26. Beliatas, M.J.; Henley, S.J.; Silva, S.R.P. Engineering the plasmon resonance of large area bimetallic nanoparticle films by laser nanostructuring for chemical sensors. *Opt. Lett.* **2011**, *36*, 1362–1364. [[CrossRef](#)] [[PubMed](#)]
27. Sharma, M.; Pudasaini, P.R.; Ruiz-Zepeda, F.; Vinogradova, E.; Ayon, A.A. Plasmonic Effects of Au/Ag Bimetallic Multispiked Nanoparticles for Photovoltaic Applications. *ACS Appl. Mater. Interfaces* **2014**, *6*, 15472–15479. [[CrossRef](#)]
28. Heinz, M.; Srabionyan, V.V.; Avakyan, L.A.; Bugaev, A.L.; Skidanenko, A.V.; Kaptelinin, S.Y.; Ihlemann, J.; Meinertz, J.; Patzig, C.; Dubiel, M.; et al. Formation of bimetallic gold-silver nanoparticles in glass by UV laser irradiation. *J. Alloy Compd.* **2018**, *767*, 1253–1263. [[CrossRef](#)]
29. Lu, C.-H.; Lan, C.-C.; Lai, Y.-L.; Li, Y.-L.; Liu, C.-P. Enhancement of green emission from InGaIn/GaN multiple quantum wells via coupling to surface plasmons in a two-dimensional silver array. *Adv. Funct. Mater.* **2011**, *21*, 4719–4723. [[CrossRef](#)]
30. Lin, C.-H.; Su, C.-Y.; Kuo, Y.; Chen, C.-H.; Yao, Y.-F.; Shih, P.-Y.; Chen, H.-S.; Hsieh, C.; Kiang, Y.-W.; Yang, C.C. Further reduction of efficiency droop effect by adding a lower-index dielectric interlayer in a surface plasmon coupled blue light-emitting diode with surface metal nanoparticles. *Appl. Phys. Lett.* **2014**, *105*, 101106. [[CrossRef](#)]
31. Jiang, S.; Hu, Z.; Chen, Z.; Fu, X.; Jiang, X.; Jiao, Q.; Yu, T.; Zhang, G. Resonant absorption and scattering suppression of localized surface plasmons in Ag particles on green LED. *Opt. Express* **2013**, *21*, 12100–12110. [[CrossRef](#)] [[PubMed](#)]
32. Yamamoto, K.; Han, D.-P.; Ishimoto, S.; Mano, R.; Kamiyama, S.; Takeuchi, T.; Iwaya, M.; Akasaki, I. Optimization of indium-tin-oxide layer thickness for surface-plasmon-enhanced green light-emitting diodes. *Jpn. J. Appl. Phys.* **2019**. Accepted.
33. Yao, Y.-C.; Hwang, J.-M.; Yang, Z.-P.; Haung, J.-Y.; Lin, C.-C.; Shen, W.-C.; Chou, C.-Y.; Wang, M.-T.; Huang, C.-Y.; Chen, C.-Y.; et al. Enhanced external quantum efficiency in GaN-based vertical-type light-emitting diodes by localized surface plasmons. *Sci. Rep.* **2016**, *6*, 22659. [[CrossRef](#)] [[PubMed](#)]
34. Fadil, A.; Iida, D.; Chen, Y.; Ma, J.; Ou, Y.; Petersen, P.M.; Ou, H. Surface plasmon coupling dynamics in InGaIn/GaN quantum-well structures and radiative efficiency improvement. *Sci. Rep.* **2014**, *4*, 6329. [[CrossRef](#)] [[PubMed](#)]

35. Yeh, D.-M.; Huang, C.-F.; Chen, C.-Y.; Lu, Y.-C.; Yang, C.C. Localized surface plasmon-induced emission enhancement of a green light-emitting diode. *Nanotechnology* **2008**, *19*, 345201. [[CrossRef](#)]
36. Tanaka, D.; Imazu, K.; Sung, J.; Park, C.; Okamoto, K.; Tamada, K. Characteristics of localized surface plasmons excited on mixed monolayers composed of self-assembled Ag and Au nanoparticles. *Nanoscale* **2015**, *7*, 15310–15320. [[CrossRef](#)] [[PubMed](#)]



© 2019 by the authors. Licensee MDPI, Basel, Switzerland. This article is an open access article distributed under the terms and conditions of the Creative Commons Attribution (CC BY) license (<http://creativecommons.org/licenses/by/4.0/>).